Multiple dating approaches applied to the recent sediments in the Yangtze River (Changjiang) subaqueous delta

Feng Wang,[1] Xiaomei Nian,[1] (iD) Jinlong Wang,[1] Weiguo Zhang,[1] Guyu Peng,[1] Can Ge,[1] Chenyin Dong,[2] (iD) Jianguo Qu[1] and Daoji Li[1]

Abstract

The accumulation rate of recent deposits in a delta environment is critical to the study of delta dynamics and their sustainable management. The most commonly used dating approach for recent (<100 years) deposits is based on radionuclide analyses (e.g. ^{210}Pb, ^{137}Cs and $^{239+240}Pu$), while alternative techniques, such as microplastics dating, are emerging. In this study, a 180-cm sediment core from the Yangtze River (Changjiang) subaqueous delta was dated using multiple techniques, including ^{210}Pb, ^{137}Cs, $^{239+240}Pu$ geochronology, microplastics content, and optically stimulated luminescence (OSL) dating. The radionuclide profiles show an irregular profile of ^{210}Pb, while $^{239+240}Pu$ exhibit a clear peak of activity at 74 ± 2 cm, which is linked to the maximum global fallout in 1963. Microplastics were not detected below a depth of 90 cm with maximum counts occurring in the top 16 cm. OSL analysis was conducted on the dominant grain size of the quartz (around 4–11 µm) and the ages were ~60 years older than those derived from ^{210}Pb, ^{137}Cs, $^{239+240}Pu$, and microplastics analyses. We infer that the relatively old quartz OSL ages are most likely caused by residual OSL signals arising from poorly bleached grains at the time of deposition. The profiles of ^{210}Pb, ^{137}Cs and $^{239+240}Pu$ activities, microplastics content, and OSL ages indicate a variable sedimentation rate over the last ~200 years reflecting the dynamic nature of delta deposits. This study shows that both OSL and microplastics particles are promising dating tools for recent young deltaic sediments, and their combined use, alongside radionuclide methods, increases the reliability of age determination.

Introduction

Deltas are a product of land-ocean interactions, which are influenced by global climate change and human activities. During recent centuries, the deltas of the world have experienced significant changes because of human activities in their catchments (Syvitski et al., 2009). The Yangtze River (Changjiang) is the third largest river in the world and historically has delivered huge amounts of sediment (~410 Mt/a, 1950–2002) into the Yangtze River estuary (Yang et al., 2014). With the operation of the Three Gorges Dam and other human activities in the catchment, sediment delivery to the Yangtze River estuary has declined significantly (Yang et al., 2014) and a great deal of attention has been given to the study of possible erosion of its subaqueous delta. The deltaic deposition/erosion rate on the time scale of decades to hundred years is commonly assessed using ^{210}Pb, ^{137}Cs, and $^{239+240}Pu$ dating techniques (Demaster et al., 1985; Huh and Su, 1999; Pan et al., 2011; Su and Huh, 2002; Wang et al., 2013, 2017a; Wei et al., 2007). However, it has also been found that excess ^{210}Pb profiles in some cores show an irregular trend with depth, which makes ^{210}Pb dating problematic (Wei et al., 2007). The artificial radionuclides ^{137}Cs and $^{239+240}Pu$ primarily provide two time-markers in a sediment core: one corresponding to the first introduction of ^{137}Cs and $^{239+240}Pu$ into the environment in 1952; the second to their maximum global fallout in 1963. However, the 1963 peaks are not always apparent in cores, and the depth of penetration of radionuclides (especially ^{137}Cs) can be much deeper or shallower than expected (Wang et al., 2013, 2016; Wei

et al., 2007). This phenomenon is most probably caused by bio-physical disturbance because of the dynamic feature of subaqueous deltas (Demaster et al., 1985; Wang et al., 2016; Yang et al., 2014). Therefore, independent dating techniques are crucial in verifying radionuclide dating results.

The optically stimulated luminescence (OSL) technique has been widely used to estimate the ages of sediments from various environments (e.g. Duller, 2004; Huntley et al., 1985). In certain environments, OSL dating can date deposits back to several hundreds of thousands of years (Rhodes, 2011; Wintle, 2008; Wintle and Murray, 2006). However, the technique has also been used to date recent sediments of several decades to several hundreds of years old (Costas et al., 2012; Kunz et al., 2014; Madsen and Murray, 2009; Medialdea et al., 2014; Muñoz-Salinas et al., 2016; Reimann et al., 2010; Shen and Mauz, 2012; Tylmann et al., 2013). For example, through a comparison of OSL and ^{210}Pb

[1]State Key Laboratory of Estuarine and Coastal Research, East China Normal University, China
[2]Department of Environmental Sciences, Faculty of Science and Engineering, Macquarie University, Australia

Corresponding author:
Xiaomei Nian, State Key Laboratory of Estuarine and Coastal Research, East China Normal University, Shanghai 200062, China.
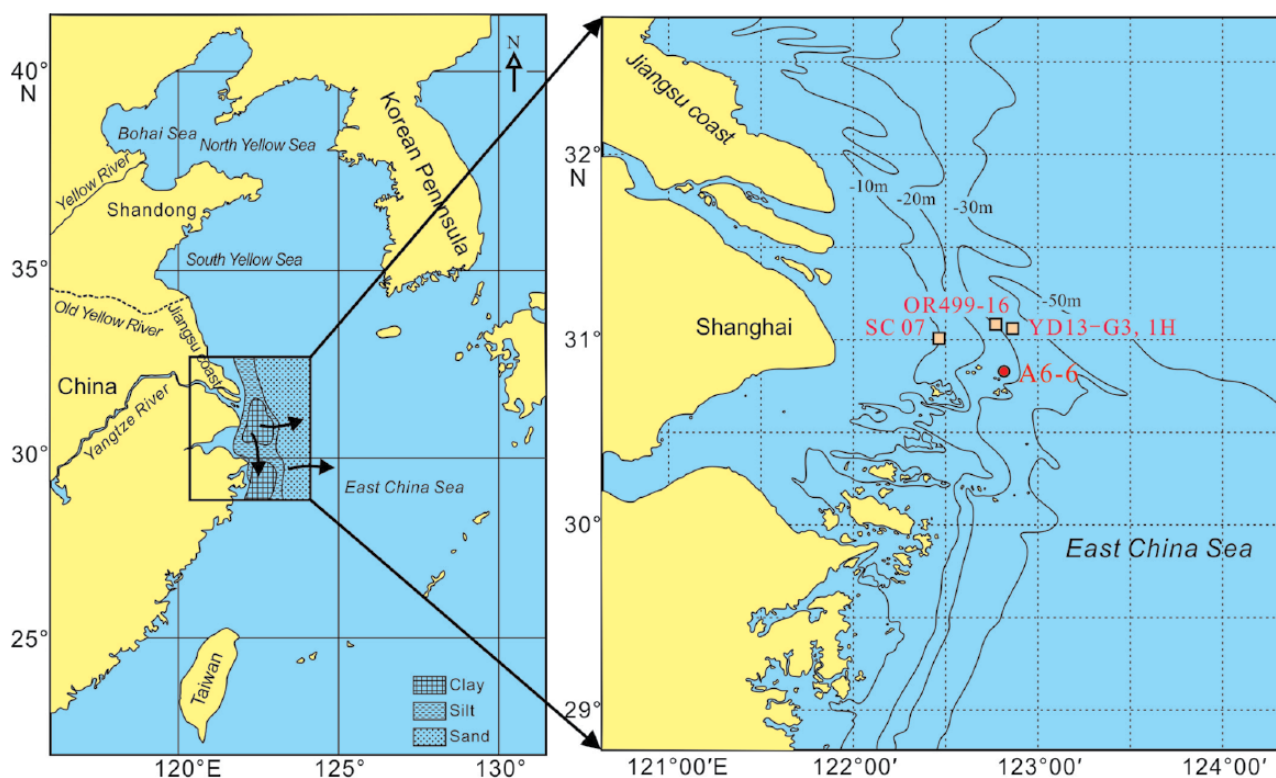Email: xmnian@sklec.ecnu.edu.cn

Figure 1. The Yangtze River delta and the location of core A6-6, and cited cores OR499-16 (Su and Huh, 2002), SC07 (Pan et al., 2011), YD13-G3 and YD13-1H (Sugisaki et al., 2015).

dating, Madsen et al. (2005, 2007) concluded that OSL dating of fine-grained estuarine sediments had a dating error of a few years for ca. 100-year-old sediment in the Wadden Sea. However, a considerable number of recent OSL samples suffer from problems of incomplete bleaching, resulting in the over estimation of ages and larger errors (Hu et al., 2010; Jain et al., 2004; Shen and Mauz, 2012). In the Yangtze River subaqueous delta, OSL dating has been used to date Holocene deposits (Sugisaki et al., 2015; Wang et al., 2015). However, the technique has not been used to date recent sediments spanning the past several hundred years. Therefore, it has been recommended that OSL dating of recent sediments should be undertaken in combination with other, independent methods such as radionuclide dating (Madsen et al., 2005, 2007).

In recent years, microplastics have been found to occur widely in lakes, estuaries and coastal areas (Claessens et al., 2011; Su et al., 2016; Zhao et al., 2014). Unlike exposure to sunlight on land, the degradation of plastics is largely retarded in the marine environment (Andrady, 2011). Once released into the sea, microplastics can remain in the marine environment for hundreds of years before mineralization because of the reduced UV light and lower temperatures (Thompson et al., 2004). Therefore, the accumulation of microplastics in sediments can be used to estimate sediment accumulation. Since microplastics are mainly derived from the plastic products used on land, we can assume that the number of microplastics found at a certain depth of sediments is related to the level of plastic production when the sediments were deposited, if other conditions (e.g. hydrodynamics, sedimentation rate) are kept the same. It has been suggested that microplastics may provide another age marker for recent sediments (Claessens et al., 2011; Zalasiewicz et al., 2016).

In this study, we discuss the use of multiple dating techniques, including ^{210}Pb, ^{137}Cs, $^{239+240}Pu$, OSL, and microplastics methods, to date recent Yangtze River subaqueous delta deposits. The purposes of the study are two-fold. First, it aims to test the OSL technique and the emerging microplastics method in dating the recent deltaic sediments. Second, since radionuclide techniques are capable of dating over ~100 years, while OSL may provide dates more than 100 years, the combination of these approaches may provide a more robust dating tool over the last several hundred years. The multiple approaches used in this study are potentially applicable to other delta environments.

Material and methods

Study area and sampling

The Yangtze River forms a substantial subaqueous delta near the river mouth. According to previous studies, the northern part of the subaqueous delta receives less deposition than its southern part, with the modern depo-center located around 31°N and 122°30′E (Chen and Shen, 1988; Demaster et al., 1985; Milliman et al., 1985). The sedimentation rate of the southern part of subaqueous delta ranges over several centimeter per year with maximum rates as high as ~6 cm/yr on a centennial scale (Demaster et al., 1985; Wei et al., 2007).

A 180 cm gravity core (A6-6, 30°48′12″N, 122°48′27″E, ~26 m water depth) was collected in 2015 (Figure 1). The sediments are generally dark black in color and consist mainly of silts. Four OSL samples were collected at depths of 160–174, 120–134, 76–90, and 30–44 cm under subdued red light. The rest of the samples were sectioned at 4 cm interval throughout the core and dried at 40°C. A total of 45 samples were subjected to particle size analysis, while 27 samples were subjected to ^{210}Pb and ^{137}Cs analysis according to the detectability of radionuclides. Based on the results of ^{210}Pb and ^{137}Cs analysis, 19 samples with detectable ^{137}Cs activities were selected for further $^{239+240}Pu$ analysis. Microplastics were analyzed at intervals of 8 cm.

Particle size measurement

Sediment particle size distribution was analyzed using a laser size analyzer (Beckman Coulter LS13-320) after treatment with 5%

H_2O_2 and 0.2 M HCl to dissolve organic matter and carbonates, respectively (Lu, 2000).

Radionuclides measurement

For ^{210}Pb and ^{137}Cs activity determination, samples were sealed in holders for 3 weeks to establish a secular equilibrium between [226]Ra and the daughter products of [222]Rn and then counted for 24 h using a hyper pure germanium (HPGe) gamma ray spectrometer (GWL-120210S). The activities of ^{210}Pb and [226]Ra ([214]Pb) were determined from gamma emissions at 46.5 (4.25%) and 351.9 keV (37.6%), respectively, with the latter used as the supported [210]Pb. Excess ^{210}Pb was calculated as the difference between total ^{210}Pb and [226]Ra. [137]Cs was determined from gamma emissions at 661.6 keV (85%).

An aliquot of 3 g dry sediment samples were ashed overnight at 450°C. After being spiked with 2–3 mBq [242]Pu (NISTSRM-4334/g), the residue containing Pu was leached with 16 M HNO_3 at 80°C for 20 h. Pu was separated from the leached solution using TEVA (100–150 μm) (Ketterer et al., 2002). The measurement of Pu was conducted using high-resolution inductively coupled plasma mass spectrometry (HR-ICP-MS) (Element II, Thermo Fisher Scientific, Waltham, MA) equipped with an ultrasonic nebulizer (Aridus II, CETAC, USA). The masses of [239]Pu and [240]Pu in the sediment samples were determined by isotope dilution calculations and then converted into the summed [239 + 240]Pu activity. The detection limit of [239 + 240]Pu was calculated as 0.002 Bq/kg based on the procedural blank for a nominal 3 g of sediment samples. A certified reference material (IAEA-385, marine sediment) was analyzed with the samples, and the analytical results of [239]Pu and [240]Pu agree well with the certified values.

Microplastics dating

The extraction technique for separating microplastics from sediments was modified from Thompson et al. (2004). To prevent airborne contamination, cotton lab coat and gloves were always worn during laboratory experiments within a room with closed windows. Glass equipment was employed wherever possible. Briefly, 50 g dry sediment was treated with 30% H_2O_2 to degrade organic matter. For the separation of the microplastics, a concentrated saline solution (1.2 g/mL) was added to the beaker and manually stirred with a clean glass rod for 2 min. The supernatant was settled for 24 h before it was passed through a filter (Whatman GF/B). Finally, the filter paper was dried at 40°C for 24 h before microscopic inspection. Microplastics were then counted under a fluorescence dissecting microscope (Leica M165 FC, Germany). To identify the microplastics, microscopic Fourier transform infrared spectroscopy (micro-FT-IR) was carried out using Thermo Fisher Nicolet iN10 (USA). Spectra were obtained to compare with libraries in the OMNIC™ Picta™ software.

OSL dating

As the sediments from core A6-6 are dominated by silts (Figure 2) and OSL dating has been successfully applied to fine-grained (4–11 μm) quartz from subaqueous delta sediments from the Yangtze River Estuary (Sugisaki et al., 2015; Wang et al., 2015), this size range of quartz grains was extracted for OSL dating. Samples preparation and OSL measurements were performed under subdued red light conditions using standard methods (Aitken, 1998). At least a 3 cm external layer was removed from block samples to ensure no contamination by grains exposed to daylight during sampling. The four samples taken from core A6-6 were treated with H_2O_2 (30%) and HCl (10%) to remove organic material and carbonates, respectively. The 4–11 μm fraction was separated by settling using the Stokes' Law. Fine-grained quartz
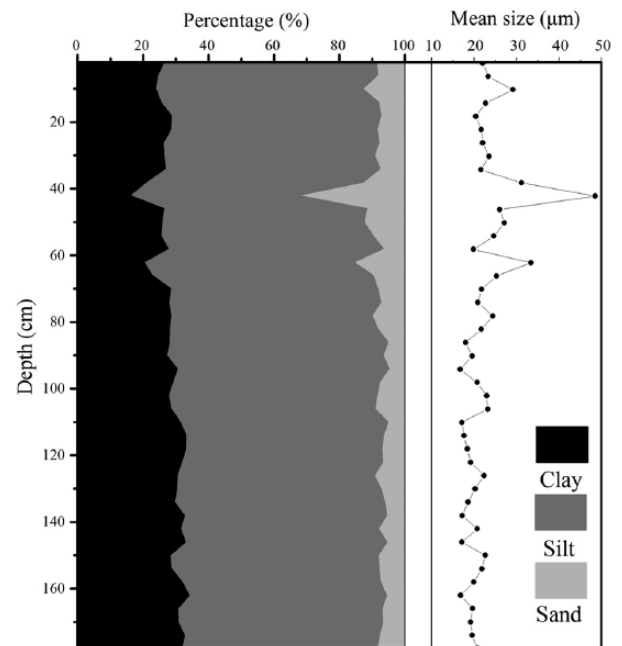

Figure 2. Down-core variations in particle size composition and mean size.

was extracted by treating polymineral extracts with silica-saturated hydrofluorosilicic acid (H_2SiF_6) (30%) for 3 days, and then rinsed in 10% HCl for 1 h and washed several times with distilled water. The purity of the quartz separate was checked by monitoring IRSL measurement and the 110°C TL peak (Li et al., 2002)

All luminescence measurements were carried out on an automated Risø TL/OSL DA-20 DASH reader (Bøtter-Jensen et al., 2003) with a 7.5-mm Hoya U-340 filter (290–370 nm) in front of an ET EMD-9107 photomultiplier tube. A calibrated ^{90}Sr/^{90}Y beta source was used for laboratory irradiation. Quartz grains were stimulated with blue light LED stimulation (470 ± 30 nm) set at 90% of 97 mW/cm^{2} full power.

The single-aliquot regenerative-dose (SAR) (Murray and Wintle, 2000) protocol was used to determine the equivalent dose (D_e) of the sediments. A preheat temperature of 200°C (10 s) and cut-heat of 160°C (0 s) was used to measure the equivalent dose in quartz. The initial 0.48 s of the signals, minus a background estimated from the average signal between 0.48 and 1.44 s (Ballarini et al., 2007), was used for D_e estimation using a single saturating exponential function, to ensure that the signal is dominated by the fast component. The water content was measured in fresh sediment immediately after opening the core, and determined by the sample weights before and after drying (weight of water/weight of dry sediment) with an average error of 5%. Concentrations of uranium (U), thorium (Th), and potassium (K) were estimated using neutron activation analysis (NAA), and the elemental concentrations are converted in dose rates using the conversion factors of Adamiec and Aitken (1998). Dose rate and OSL ages were calculated using DRAC-Calculator 1.2 (Durcan et al., 2015). An alpha efficiency factor (*a*-value) of 0.04 ± 0.02 for quartz (Rees-Jones, 1995) was used for the calculation of the dose rates. Alpha and beta dose rates were calculated using Brennan et al. (1991) and Guérin et al. (2012) attenuation factors, respectively.

Results

Particle size distribution

The particle size of core A6-6 is quite similar throughout its length except for two coarser layers at depths of 60–64 cm and 40–44 cm (Figure 2). It is dominated by silt (4–63 μm), which ranges from
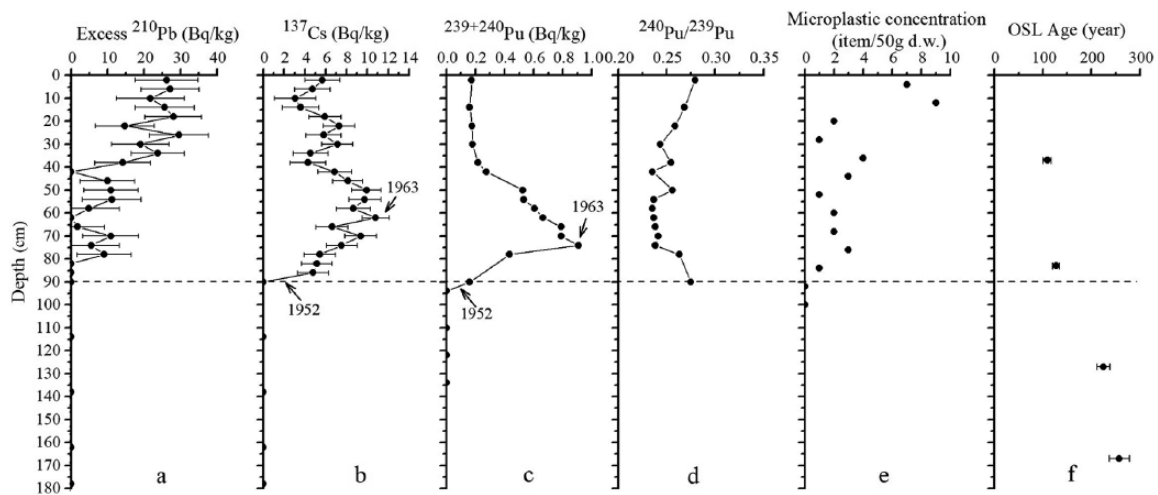
Figure 3. Down-core variations in excess (a) ^{210}Pb, (b) ^{137}Cs, (c) $^{239 + 240}$Pu activity, (e) ^{240}Pu/^{239}Pu ratio, (e) microplastics concentration, (f) and OSL age.

51% to 68% with a mean value of 63%. Clay (<4 μm) ranges from 16% to 34% with a mean value of 28%, and sand (>63 μm) 5–33% with a mean value of 9%. The mean particle size of core A6-6 falls between 17 and 49 μm, with a mean value of 23 μm.

Radionuclides distribution

The distribution of excess ^{210}Pb and ^{137}Cs are shown in Figure 3a and b. Excess ^{210}Pb values and ^{137}Cs are not detectable below depths of 76–80 and 84–88 cm, respectively. From the 76–80 cm layer to the surface, an upward increasing trend of ^{210}Pb activity is shown. If the constant initial concentration (CIC) model (Appleby and Oldfield, 1978) is applied to the upper 56 cm, a mean sedimentation rate of 0.32 ± 0.06 cm/yr ($R^2 = 0.62$) is derived. From 88 cm to 60 cm depth, there is an upward increasing trend in ^{137}Cs activity with a peak (10.81 Bq/kg) at 62 ± 2 cm. $^{239 + 240}$Pu activity is not detected below 92 cm depth. From 92 to 72 cm depth, there is a rapid upward increasing trend with a peak (0.907 Bq/kg) at 74 ± 2 cm depth. There is a declining trend from 72 to 48 cm depth, which remains low and stable from 48 cm to the surface (Figure 3c). The ^{240}Pu/^{239}Pu atom ratio ranges between 0.236 and 0.279. It decreases gradually from 92 to 28 cm depth and then increases to the surface (Figure 3d).

Microplastics distribution

The number of microplastics is shown in Figure 3e. A total of 35 microplastic particles were found in 550 g of sediment core samples. The most abundant shapes of the microplastics are fibers (28 particles), followed by fragments (4 particles) and pellets (3 particles). Transparent particles (17 particles) and blue particles (14 particles) are the main colors of the microplastics with four purple particles observed. Images of selected microplastics are shown in Figure 4. Microplastics occur first at 84 cm in depth at 1 particle per 50g dry sediment (20 n/kg). The number of microplastics ranges between 1 and 4 particles per 50 g dry sediment from 88 to 16 cm depth. The maximum value was found at the top part of the core: nine particles at 4–16 cm depth (180 n/kg) and seven particles at 0–8 cm depth (140 n/kg). The microplastic particles (>600 μm) from 40 to 48 cm has been identified as polyester according to the micro-FT-IR analysis (Figure 4e).

OSL dating

As shown in Figure 5a, a preheat plateau test was carried out on sample L84 in order to select an appropriate preheat temperature

in the range of 160°C to 300°C, with a cut-heat temperature of 160°C, for the SAR protocol with at least three aliquots measured at each temperature. Based on this experiment, a preheat temperature of 200°C for 10 s and a cut-heat of 160°C for 0 s were selected for routine dose measurements.

A dose recovery experiment (Murray and Wintle, 2003) was performed on sample L84 using the SAR protocol. The natural signal of the samples was bleached using a Hönle SOL2 solar simulator for 1 h. Following the bleaching, a known laboratory beta dose of 0.71 Gy with a test dose of 0.71 Gy was given to the sample; the measured-to-given dose ratio is 1.009 ± 0.1 ($n = 6$). The recycling ratios and recuperation values of all data were within 0.90–1.10 and <2%, respectively. The rapid decay of the signals with stimulation time indicated that the signals were dominated by the fast component (Figure 5b). The above results indicated that the SAR protocol is suitable for equivalent dose determination for the samples from the Yangtze River subaqueous delta (Figure 5c).

A summary of the depth, water content, dose rate, D_e values and ages of the samples is shown in Table 1. The OSL ages range from 109 ± 9 to 258 ± 21 years, and these internally consistent OSL ages increase with depth (Figure 3f)

Discussion

A comparison of radionuclide, microplastics and OSL ages

The sedimentation rates estimated from ^{210}Pb$_{ex}$ using a CIC model are valid only if the sediment deposition rate has not changed within the past hundred years (Appleby and Oldfield, 1978). According to the CIC model, we obtain a linear sedimentation rate of 0.32 ± 0.06 cm/yr in core A6-6. However, the core is located near the river mouth, where sediment reworking, erosion, and increasing anthropogenic activities during the past two decades make the Yangtze Estuary a dynamic environment (Luan et al., 2016; Wang et al., 2016; Zhu et al., 2016). Thus, the ^{210}Pb$_{ex}$ estimated sedimentation rate for core A6-6 may be unreliable and is significantly lower than the 1.3–1.9 cm/yr reported for cores from neighboring sites (Pan et al., 2011; Su and Huh, 2002). This phenomenon was also reported in previous studies (Pan et al., 2011; Wang et al., 2016) and attributed to the dynamic sedimentary environment of the Yangtze River delta (Luan et al., 2016; Yang et al., 2014). However, this sedimentary environment was relatively steady before the 1980s, and thus the time-markers (^{137}Cs and $^{239 + 240}$Pu) in 1963 and 1952 perhaps can be used to determine sedimentation rates in this region. Based on the penetration depth of
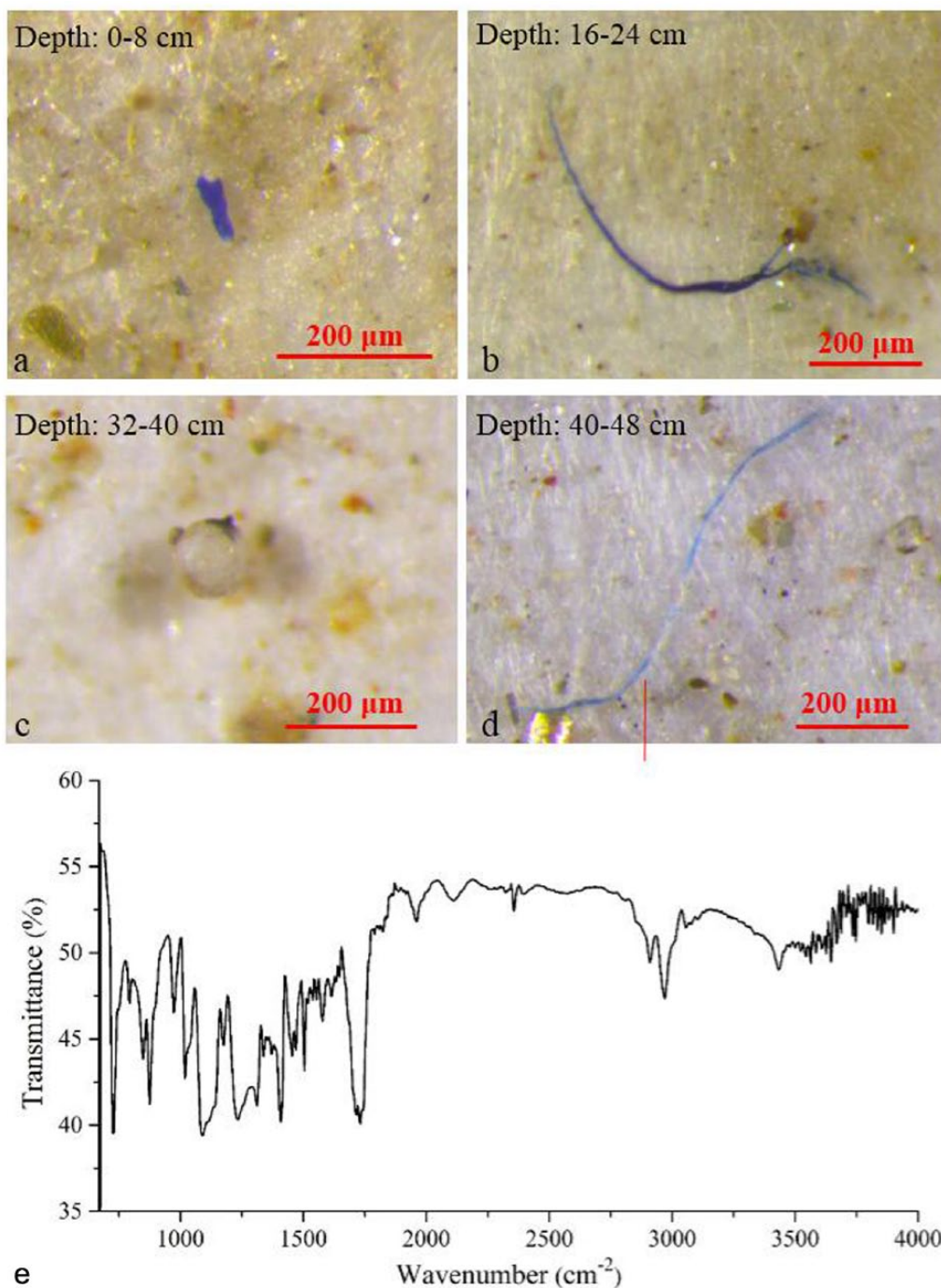
Figure 4. (a–d) Images of microplastics and the (e) spectrum of microplastics at 40–48 cm depth which was identified as polyester (match: 86.32) using micro-FT-IR.

[137]Cs and [239 + 240]Pu at 90 ± 4 cm (Figure 3b and c), we estimate a mean sedimentation rate of 1.43 ± 0.08 cm/yr since 1952. The peak layer of [239 + 240]Pu corresponding to the year 1963 ± 1 allows us obtain a sedimentation rate of 1.42 ± 0.07 cm/yr for the layer above 74 ± 2 cm. The less sharp peak of ^{137}Cs occurs at a shallower depth of 62 ± 2 cm, which was probably caused by the mobility of ^{137}Cs in the marine environment broadening this feature (Foster et al., 2006; Wang et al., 2017a, 2017b). Different depths for peak ^{137}Cs and [239 + 240]Pu have also been reported for a nearby core (Liu et al., 2011). This rate is also of similar magnitude to those obtained from nearby cores, for example, 1.3–1.9 cm/yr in core SC07 (Pan et al., 2011) and 1.7–1.8 cm/yr in core OR499-16 (Su and Huh, 2002) (Figure 1). A number of studies have suggested that Pu in the Yangtze Estuary was mainly derived from inputs from the Yangtze River and Pacific Proving Grounds (PPG), which were characterized by a [240]Pu/[239]Pu atomic ratio of 0.18 and 0.33–0.36

(e.g. Pan et al., 2011; Wang et al., 2017a), respectively. The higher atomic ratios observed in the 88–92 cm layer (Figure 3d) is closer to the PPG signal, which suggests the significant influence of this input in the 1950s (Zheng and Yamada, 2004). It further confirms the [239 + 240]Pu activity-based sedimentation rate. The increasing trend of the [240]Pu/[239]Pu atomic ratio in top 24 cm of the core reflects the decreased global fallout of Pu and sediment discharge of the Yangtze River after 2000 (Yang et al., 2014), which consequently has decreased the terrigenous signal of [240]Pu/[239]Pu, but increased the relative contribution of PPG sourced Pu (Zheng and Yamada, 2004).

In core A6-6, microplastics occur first at a depth of 84 cm. The surface content (7 particles per 50 g dry sediment) is very close to the mean value (6 particles per 50 g dry sediment) from the Yangtze River subaqueous delta (Peng et al., 2017). Globally, plastics production started in the early 1900s and its production in China is
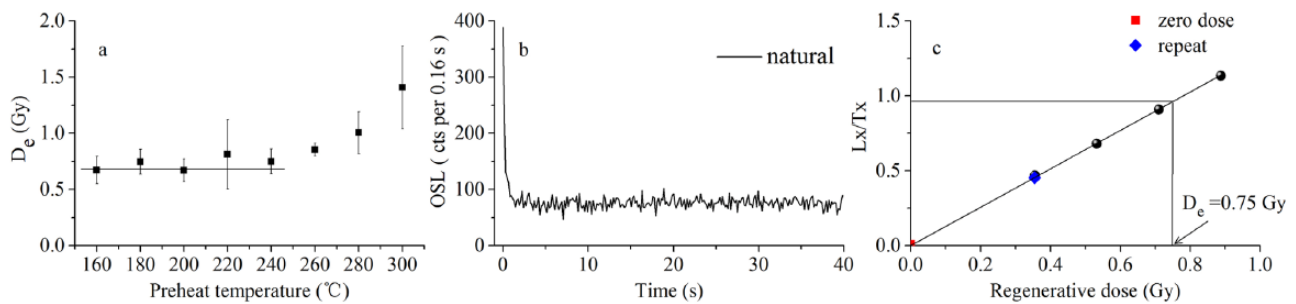
Figure 5. (a) Preheat plateau test, (b) decay curve, and (c) growth curve obtained with the SAR protocol using fine-grained quartz from sample L84.

dated to the 1920s. The record of China's annual plastics production (CPCIA, 1984–2014) shows that levels were relatively low before the 1950s (Figure 6). Given the massive change in plastic production and usage in China this record shows, we suggest that the age of sediment at 84 cm lies around the 1950s. According to the OSL dating, the ages of the sediments below 90 cm are older than 100 years and sediments above 90 cm were deposited within the last 130 years. However, if we compare the OSL ages with ^{137}Cs, $^{239+240}$Pu, and microplastics dating, it seems that the OSL ages are ~60 years older than the ages estimated by the radionuclide and microplastics methods. The ~60 years age discrepancy between the OSL and the radionuclide techniques, as well as the microplastics methods, may be related to the problem of incomplete bleaching in the OSL dating for recent deposits (Madsen and Murray, 2009). A number of studies have found that incomplete bleaching is more pronounced in fine-grained quartz (Hu et al., 2010; Jain et al., 2004; Shen and Mauz, 2012). One possible reason is that finer grains tend to coagulate and form larger aggregates during transportation (Hu et al., 2010). In the Mississippi delta, a residual OSL age of ~100 year is reported (Shen and Mauz, 2012), and this phenomenon may also be applied to other large river deltas in the world. In Sugisaki's study of Holocene deposits in the subaqueous delta of the Yangtze River, they found that modern suspended particulate matter in the near-surface water of the Yangtze River had a measured quartz equivalent dose between 0.1 and 0.2 Gy, which equals about 60 years (Sugisaki et al., 2015). This value may not have significant effects on a chronology on a millennial scale, but its effect cannot be neglected on a century time scale. If we deduct 60 years from our OSL ages, we derive a more appropriate result, which is very close to the microplastics, ^{137}Cs and $^{239+240}$Pu ages (Figure 7). This study therefore further demonstrates that residual OSL signals should be properly addressed in dating recent deposits. In the following discussion, the OSL ages after subtracting 60 years were used.

In summary, radionuclide, microplastics, and OSL methods can be usefully combined to determine the age of sediment deposited over the past ~100 years. The ^{137}Cs and $^{239+240}$Pu fallout peaks in 1963 can normally provide useful time-markers. However, microplastics dating is an emerging dating tool and more work is needed to improve its age accuracy. Compared with other methods, the counting of microplastics does not require expensive instruments. Because of the wide occurrence of microplastics in the sediments, this method can potentially have widespread use in dating recent sediments. The OSL method complements the radionuclide methods in that it can provide ages of sediments older than 100 years.

Temporal variation of sedimentation rate

An age–depth model implemented using the Bacon (version 2.2) software package (Blaauw and Christen 2011) was used to reconstruct accumulation histories of the deposits. The software divides the core into many thin vertical sections, and accumulation rates for each of these sections are estimated by the Markov Chain Monte Carlo (MCMC) iterations. The age model including the dating results from the different methods is shown in Figure 7. Considering the uncertainty (4 cm in radionuclide dating and 7 cm in OSL dating) because of sedimentary particle compaction during sub-sectioning and the transport time (1.0 year) from the PPG to the East China Sea (ECS) sediment, the mean sedimentation rate according to the radionuclide event markers for the top 90 cm is estimated to be 1.42 ± 0.07 cm/yr. From 83 to 127 cm, the corrected OSL ages yield a mean sedimentation rate about 0.45 ± 0.22 cm/yr. From 127 to 167 cm, the sedimentation rate rises again to ~1.2 cm/yr. Such a transition means that sediment deposition rates clearly vary with time reflecting the dynamic nature of the sedimentary environment.

The time variation in the sedimentation rates can be linked to variations in sediment supply and hydrodynamics. The relative

Table 1. U, Th, K concentration, D_e, OSL ages of the samples collected from the core A6-6.

Lab no.	U (ppm)	Th (ppm)	K (%)	Depth (cm)	Water (%)	No. of aliquots
L81	2.24 ± 0.09	12.30 ± 0.34	2.30 ± 0.07	37 ± 7	53 ± 5	12
L82	2.49 ± 0.10	13.30 ± 0.36	2.40 ± 0.07	83 ± 7	47 ± 5	12
L83	2.28 ± 0.09	11.10 ± 0.31	2.42 ± 0.07	127 ± 7	49 ± 5	14
L84	2.49 ± 0.10	13.20 ± 0.36	2.57 ± 0.07	167 ± 7	49 ± 5	11

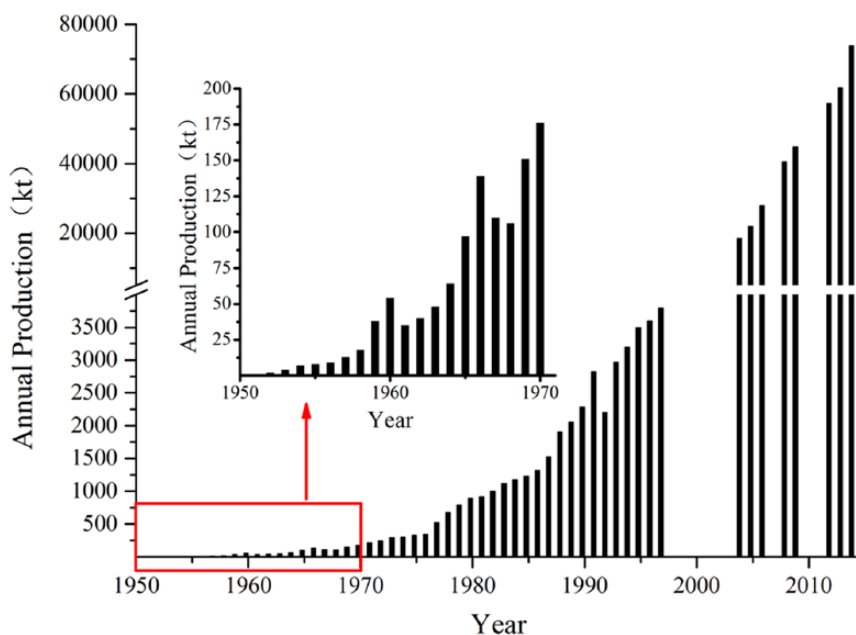| Lab no.	D_e (Gy)	Environment al dose rate (Gy/ka)					Age (a)
		Alpha	Beta	Gamma	Cosmic	Total	
L81	0.29 ± 0.02	0.29 ± 0.11	1.47 ± 0.07	0.87 ± 0.04	0.025 ± 0.002	2.66 ± 0.13	109 ± 9
L82	0.38 ± 0.01	0.34 ± 0.12	1.63 ± 0.08	0.98 ± 0.04	0.024 ± 0.002	2.96 ± 0.15	128 ± 7
L83	0.62 ± 0.02	0.29 ± 0.10	1.56 ± 0.07	0.88 ± 0.04	0.024 ± 0.002	2.75 ± 0.13	225 ± 13
L84	0.78 ± 0.05	0.33 ± 0.12	1.68 ± 0.08	0.98 ± 0.04	0.023 ± 0.002	3.02 ± 0.15	258 ± 21

Figure 6. Annual plastic production in China (CPCIA, 1984–2014).

lower sedimentation between 127 and 83 cm could be linked to the northern shift of the Yellow River in AD 1855 (Zhang, 1984). It has been demonstrated that the Yellow River discharge into the Yellow Sea between AD 1128 and 1855. It forms a delta at the northern part of the Jiangsu coast. At the same time, it also supplies sediments to the Yangtze River delta (Liu et al., 2010; Zhang et al., 2012). When the Yellow River shifted back to the Bohai Sea in northern China in AD 1855, it is expected that the sediment supply from the former Yellow River delta will have been reduced, impacting the sedimentation rate at the study site accordingly. The OSL corrected age at 127 ± 7 cm depth is 165 ± 13 years (AD 1850 ± 13), which coincides well with the timing of the shift of the Yellow River. The data indicate that sediment loads from the Yangtze River have increased since the 1950s, reaching a peak in the early 1960s. After the 1960s, there was a declining trend, which is caused by afforestation and damming, trapping sediments in the catchment (Yang et al., 2014). Although we do not have sediment load data before 1950 for the Yangtze River, the reconstructed sediment load shows that the sediment load between 1860 and 1950 is no higher than that between 1950 and 1980 (Wang et al., 2008). The top 90 cm of our core was deposited since the 1950s, indicating a higher sedimentation rate, which can be explained by increased human activities since the 1950s.

Because of the monsoon climate of the region, sediment supply from the river shows markedly seasonal changes, with most sediment delivered during the summer season. Previous studies have also indicated that the seasonal deposition rate based on ^{7}Be and ^{234}Th is much higher than that calculated by ^{210}Pb and ascribed to be the erosion of seasonal deposits on a decadal time scale (Demaster et al., 1985). Extreme events like typhoons also have an impact on delta deposition. These dynamic characteristics mean that dating delta deposits is challenging. Although radionuclide, microplastics, and OSL dating remain to be improved, their combined use could provide a more reliable approach to age determination, which is critical for the study of sediment dynamics in delta environments.

Conclusion

Multiple dating techniques, including ^{210}Pb, ^{137}Cs, $^{239 + 240}Pu$, microplastics, and OSL, have been applied to recent sediments in the Yangtze River subaqueous delta. The peaks in $^{239 + 240}Pu$ ($74 \pm$
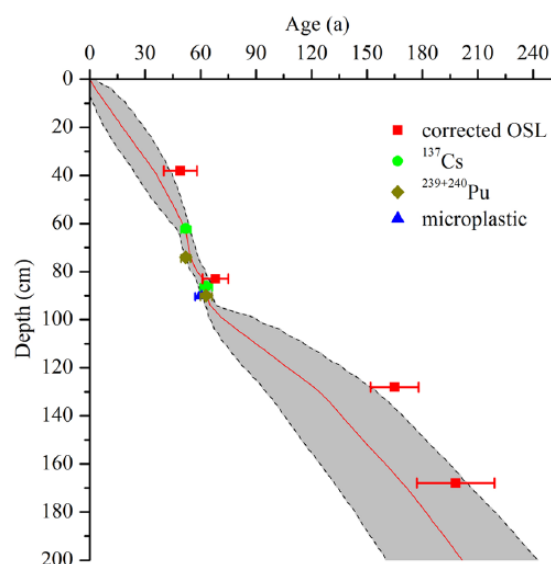

Figure 7. The age–depth model for core A6-6 generated by Bacon (Blaauw and Christen, 2011); gray dotted lines indicate 95% confidence intervals; the red curve shows the single 'best' model based on the weighted mean age for each depth. The age of the top of the core (year of coring, AD 2015) was added into the age–depth model and all the ages were relative to AD 2015 for comparison. Red squares: corrected OSL ages (after subtracting 60 years); green circles: ^{137}Cs ages; dark yellow diamonds: $^{239 + 240}Pu$ ages; blue triangles: microplastics age.

2 cm) and ^{137}Cs (62 ± 2 cm) activities mark 1963. Microplastics were only detected above a depth of 90 cm with maximum counts occurring in the top 16 cm. A comparison of the various ages obtained using different techniques indicates that OSL ages are 60 years older than the expected age, which is most probably caused by incomplete bleaching. The similarity of OSL ages over the intervals 167–127 cm and 83–37 cm implies rapid deposition over these intervals. In contrast, the 127–83 cm layer has a lower sedimentation rate. Such a variation in sedimentation with time is consistent with the dynamic nature of delta deposits. This study demonstrates that OSL and microplastics analyses are promising dating tools for recent sediments in the marine environment.

However, further studies are needed to address the residual OSL signal problems associated with delta fine-grained sediments.

ORCID iDs

Xiaomei Nian https://orcid.org/0000-0002-3164-9254
Chenyin Dong https://orcid.org/0000-0001-9566-3701

References

Adamiec G and Aitken M (1998) Dose rate conversion factors update. *Ancient TL* 16: 37–50.

Aitken M (1998) *An Introduction to Optical Dating*. New York: Oxford University Press, 347 pp.

Andrady AL (2011) Microplastics in the marine environment. *Marine Pollution Bulletin* 62: 1596–1605.

Appleby PG and Oldfield FR (1978) The calculation of lead-210 dates assuming a constant rate of supply of unsupported ^{210}Pb to the sediment. *Catena* 1: 1–8.

Ballarini M, Wallinga J, Wintle AG et al. (2007) A modified SAR protocol for optical dating of individual grains from young quartz samples. *Radiation Measurements* 42: 360–369.

Blaauw M and Christen JA (2011) Flexible paleoclimate age-depth models using an autoregressive gamma process. *Bayesian Analysis* 6: 457–474.

Bøtter-Jensen L, Andersen CE, Duller GAT et al. (2003) Developments in radiation, stimulation and observation facilities in luminescence measurements. *Radiation Measurements* 37: 535–541.

Brennan BJ, Lyons RG and Phillips SW (1991) Attenuation of alpha particle track dose for spherical grains. *International Journal of Radiation Applications and Instrumentation, Part D: Nuclear Tracks and Radiation Measurements* 18: 249–253.

Chen JY and Shen HT (1988) *Processes of Dynamics and Geomorphology of the Changjiang Estuary*. Shanghai: Shanghai Science and Technical Publication, 454 pp. (in Chinese).

Claessens M, Meester SD, Landuyt LV et al. (2011) Occurrence and distribution of microplastics in marine sediments along the Belgian coast. *Marine Pollution Bulletin* 62: 2199–2204.

Costas I, Reimann T, Tsukamoto S et al. (2012) Comparison of OSL ages from young dune sediments with a high-resolution independent age model. *Quaternary Geochronology* 10: 16–23.

CPCIA (1984–2014) *China Chemical Industry Yearbook*. Beijing: China Chemical Industry Publishing House (in Chinese).

Demaster DJ, McKee BA, Nittrouer CA et al. (1985) Rates of sediment accumulation and particle reworking based on radio-chemical measurements from continental shelf deposits in the East China Sea. *Continental Shelf Research* 4: 143–158.

Duller GAT (2004) Luminescence dating of quaternary sediments: Recent advances. *Journal of Quaternary Science* 19: 183–192.

Durcan JA, King GE and Duller GAT (2015) DRAC: Dose Rate and Age Calculator for trapped charge dating. *Quaternary Geochronology* 28: 54–61.

Foster IDL, Mighall TM, Proffitt H et al. (2006) Post-depositional ^{137}Cs mobility in the sediments of three shallow coastal lagoons, SW England. *Journal of Paleolimnology* 35: 881–895.

Guérin G, Mercier N, Nathan R et al. (2012) On the use of the infinite matrix assumption and associated concepts: A critical review. *Radiation Measurements* 47: 778–785.

Hu G, Zhang JF, Qiu WL et al. (2010) Residual OSL signals in modern fluvial sediments from the Yellow River (HuangHe) and the implications for dating young sediments. *Quaternary Geochronology* 5: 187–193.

Huh CA and Su CC (1999) Sedimentation dynamics in the East China Sea elucidated from Pb-210, Cs-137 and Pu-239, Pu-240. *Marine Geology* 160: 183–196.

Huntley DJ, Godrey-Smith DI and Thewalt MLW (1985) Optical dating of sediments. *Nature* 313: 105–107.

Jain M, Murray AS and Botter-Jensen L (2004) Optically stimulated luminescence dating: How significant is incomplete light exposure in fluvial environments? *Quaternaire* 15: 143–157.

Ketterer ME, Watson BR, Matisoff G et al. (2002) Rapid dating of recent aquatic sediments using Pu activities and ^{240}Pu/^{239}Pu as determined by quadrupole inductively coupled plasma mass spectrometry. *Environmental Science & Technology* 36: 1307–1311.

Kunz A, Pflanz D, Weniger T et al. (2014) Optically stimulated luminescence dating of young fluvial deposits of the Middle Elbe River Flood Plains using different age models. *Geochronometria* 41: 36–56.

Li SH, Sun JM and Zhao H (2002) Optical dating of dune sands in the northeastern deserts of China. *Palaeogeography, Palaeoclimatology, Palaeoecology* 181: 419–429.

Liu J, Saito Y, Kong XH et al. (2010) Sedimentary record of environmental evolution off the Yangtze River estuary, East China Sea, during the last ~13,000 years, with special reference to the influence of the Yellow River on the Yangtze River delta during the last 600 years. *Quaternary Science Reviews* 29: 2424–2438.

Liu ZY, Zheng J, Pan SM et al. (2011) Pu and Cs-137 in the Yangtze River estuary sediments: Distribution and source identification. *Environmental Science & Technology* 45: 1805–1811.

Lu RK (2000) *Soil and Agricultural Chemistry Analysis Method*. Beijing: China Agriculture Science and Technology Press, 665 pp. (in Chinese).

Luan HL, Ding PX, Wang ZB et al. (2016) Decadal morphological evolution of the Yangtze Estuary in response to river input changes and estuarine engineering projects. *Geomorphology* 265: 12–23.

Madsen AT and Murray AS (2009) Optically stimulated luminescence dating of young sediments: A review. *Geomorphology* 109: 3–16.

Madsen AT, Murray AS, Andersen TJ et al. (2005) Optically stimulated luminescence dating of young estuarine sediments: A comparison with ^{210}Pb and ^{137}Cs dating. *Marine Geology* 214: 251–268.

Madsen AT, Murray AS, Andersen TJ et al. (2007) Optical dating of young tidal sediments in the Danish Wadden Sea. *Quaternary Geochronology* 2: 89–94.

Medialdea A, Thomsen KJ, Murray AS et al. (2014) Reliability of equivalent-dose determination and age-models in the OSL dating of historical and modern palaeoflood sediments. *Quaternary Geochronology* 22: 11–24.

Milliman JD, Shen HT, Yang ZS et al. (1985) Transport and deposition of river sediment in the Changjiang estuary and adjacent continental shelf. *Continental Shelf Research* 4: 37–45.

Muñoz-Salinas E, Castillo M, Sanderson D et al. (2016) Using three different approaches of OSL for the study of young fluvial sediments at the coastal plain of the Usumacinta-Grijalva River Basin, southern Mexico. *Earth Surface Processes and Landforms* 41: 823–834.

Murray AS and Wintle AG (2000) Luminescence dating of quartz using an improved single-aliquot regenerative-dose protocol. *Radiation Measurements* 32: 57–73.

Murray AS and Wintle AG (2003) The single aliquot regenerative dose protocol: Potential for improvements in reliability. *Radiation Measurements* 37: 377–381.

Pan SM, Tims SG, Liu XY et al. (2011) ^{137}Cs, $^{239+240}$Pu concentrations and the ^{240}Pu/^{239}Pu atom ratio in a sediment core from the sub-aqueous delta of Yangtze River estuary. *Journal of Environmental Radioactivity* 102: 930–936.

Peng GY, Zhu BS, Yang DQ et al. (2017) Microplastics in sediments of the Changjiang Estuary, China. *Environmental Pollution* 225: 283–290.

Rees-Jones J (1995) Optical dating of young sediments using fine-grain quartz. *Ancient TL* 13: 9–14.

Reimann T, Naumann M, Tsukamoto S et al. (2010) Luminescence dating of coastal sediments from the Baltic Sea coastal barrier-spit Darss–Zingst, NE Germany. *Geomorphology* 122: 264–273.

Rhodes EJ (2011) Optically stimulated luminescence dating of sediments over the past 200,000 years. *Annual Review of Earth and Planetary Sciences* 39: 461–488.

Shen ZX and Mauz B (2012) Optical dating of young deltaic deposits on a decadal time scale. *Quaternary Geochronology* 10: 110–116.

Su CC and Huh CA (2002) ^{210}Pb, ^{137}Cs and $^{239;240}$Pu in East China Sea sediments: Sources, pathways and budgets of sediments and radionuclides. *Marine Geology* 183: 163–178.

Su L, Xue YA, Li LY et al. (2016) Microplastics in Taihu Lake, China. *Environmental Pollution* 216: 711–719.

Sugisaki S, Buylaert J, Murray A et al. (2015) OSL dating of fine-grained quartz from Holocene Yangtze delta sediments. *Quaternary Geochronology* 30: 226–232.

Syvitski JPM, Kettner AJ, Overeem I et al. (2009) Sinking deltas due to human activities. *Nature Geoscience* 2: 681–686.

Thompson RC, Olsen Y, Mitchell RP et al. (2004) Lost at sea: Where is all the plastic? *Science* 304: 838.

Tylmann W, Enters D, Kinder M et al. (2013) Multiple dating of varved sediments from Lake Łazduny, northern Poland: Toward an improved chronology for the last 150 years. *Quaternary Geochronology* 15: 98–107.

Wang HJ, Yang ZS, Wang Y et al. (2008) Reconstruction of sediment flux from the Changjiang (Yangtze River) to the sea since the 1860s. *Journal of Hydrology* 349: 318–332.

Wang JL, Baskaran M, Hou XL et al. (2017a) Historical changes in ^{239}Pu and ^{240}Pu sources in sedimentary records in the East China Sea: Implications for provenance and transportation. *Earth and Planetary Science Letters* 466: 32–42.

Wang JL, Baskaran M and Niedermiller J (2017b) Mobility of 137Cs in freshwater lakes: A mass balance and diffusion study of Lake St. Clair, Southeast Michigan, USA. *Geochimica et Cosmochimica Acta* 218: 323–342.

Wang JL, Du JZ, Baskaran M et al. (2016) Mobile mud dynamics in the East China Sea elucidated using ^{210}Pb, ^{137}Cs, ^{7}Be, and ^{234}Th as tracers. *Journal of Geophysical Research: Oceans* 121: 224–239.

Wang X, Shi XF, Wang GQ et al. (2013) Sedimentation rates and its indication to distribution of Yangtze sediment supply around the Yangtze (Changjiang) River Estuary and its adjacent area, China. *Earth Science: Journal of China University of Geosciences* 38: 763–775 (in Chinese with English abstract).

Wang Y, Long H, Yi L et al. (2015) OSL chronology of a sedimentary sequence from the inner-shelf of the East China Sea and its implication on post-glacial deposition history. *Quaternary Geochronology* 30: 282–287.

Wei TY, Chen ZY, Duan LY et al. (2007) Sedimentation rates in relation to sedimentary processes of the Yangtze Estuary, China. *Estuarine, Coastal and Shelf Science* 71: 37–46.

Wintle AG (2008) Fifty years of luminescence dating. *Archaeometry* 50: 276–312.

Wintle AG and Murray AS (2006) A review of quartz optically stimulated luminescence characteristics and their relevance in single-aliquot regeneration dating protocols. *Radiation Measurements* 41: 369–391.

Yang SL, Milliman JD, Xu KH et al. (2014) Downstream sedimentary and geomorphic impacts of the Three Gorges Dam on the Yangtze River. *Earth-Science Reviews* 138: 469–486.

Zalasiewicz J, Waters CN, Ivar Do Sul JA et al. (2016) The geological cycle of plastics and their use as a stratigraphic indicator of the Anthropocene. *Anthropocene* 13: 4–17.

Zhang RS (1984) Land-forming history of the Huanghe River delta and coastal plain of northern Jiangsu. *Acta Geographica Sinica* 39: 173–184 (in Chinese with English abstract).

Zhang WG, Ma HL, Ye LP et al. (2012) Magnetic and geochemical evidence of Yellow and Yangtze River influence on tidal flat deposits in northern Jiangsu Plain, China. *Marine Geology* 319–322: 47–56.

Zhao SY, Zhu LX, Wang T et al. (2014) Suspended microplastics in the surface water of the Yangtze Estuary System, China: First observations on occurrence, distribution. *Marine Pollution Bulletin* 86: 562–568.

Zheng J and Yamada M (2004) Sediment core record of global fallout and bikini close-in fallout Pu in Sagami Bay, Western Northwest Pacific Margin. *Environmental Science & Technology* 38: 3498–3504.

Zhu L, He Q, Shen J et al. (2016) The influence of human activities on morphodynamics and alteration of sediment source and sink in the Changjiang Estuary. *Geomorphology* 273: 52–62.